Catena 223 (2023) 106953

Contents lists available at ScienceDirect

Catena

journal homepage: www.elsevier.com/locate/catena

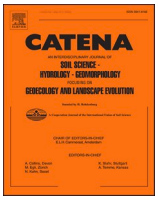

Mapping of the wind erodible fraction of soil by bidirectional gated recurrent unit (BiGRU) and bidirectional recurrent neural network (BiRNN) deep learning models

Mahrooz Rezaei [a,*], Aliakbar Mohammadifar [b], Hamid Gholami [b,*], Monireh Mina [c], Michel J.P.M. Riksen [d], Coen Ritsema [d]

[a] Meteorology and Air Quality Group, Wageningen University & Research, PO. Box 47, 6700 AA Wageningen, the Netherlands
[b] Department of Natural Resources Engineering, University of Hormozgan, Bandar-Abbas, Hormozgan, Iran
[c] Department of Soil Science, School of Agriculture, Shiraz University, Shiraz, Iran
[d] Soil Physics and Land Management Group, Wageningen University & Research, PO. Box 47, 6700 AA Wageningen, the Netherlands

ARTICLE INFO

Keywords:
Wind erosion
Neural network
Deep learning
Game theory
Uncertainty

ABSTRACT

The destructive consequences of wind erosion have been reported in many studies, but accurate assessment of wind erosion is still a challenge, especially on large scales. Our research introduces two deep learning (DL) algorithms consisting of bidirectional gated recurrent unit (BiGRU), and bidirectional recurrent neural network (BiRNN) for spatial mapping of wind-erodible fraction of the soil (EF). EF was measured in 508 soil samples using the Chepil method. 15 key factors controlling EF including: soil, topography, and meteorology parameters were mapped. The performance of the most efficient DL model was interpreted by Game theory. The uncertainty of the DL models was quantified by deep quantile regression (DQR). Results showed that both DL models were performed very well with the BiRNN performing slightly better than BiGRU. The aggregate mean weight diameter (MWD) was a key variable for the mapping of soil susceptibility to wind erosion. Based on the BiRNN model, most of the study region was moderately and highly susceptible to wind erosion regarding the EF value (between 32 and 98). This indicates the urgent need for soil conservation measures in the region. The DQR results showed that the observed values of EF fell within the EF values predicted by the model. Overall, the suggested methodology has proven to be helpful in mapping wind erosion susceptibility on a large scale.

1. Introduction

Wind erosion is a major challenge in drylands and frequently occurs in the Middle East (Shao et al., 2013). Wind erosion is a threat for the agricultural lands and air quality (Středová et al., 2021). In fact, aeolian sediment transport and wind erosion pose serious hazards to human health (Rezaei et al., 2019). It is therefore important to minimize the erosion risk and identify the areas where the wind erosion risk is high.

In comparison with the direct measurement techniques of wind erosion and soil erodibility such as wind tunnel, indirect techniques (e.g., remote sensing methods, data-based models, predictive models) are inexpensive and has been employed by some researchers (Chepil, 1962, Borrelli et al., 2014). The soil EF - aggregates < 0.84 mm - provide valuable information about the relationship between land surface properties and wind erosion (Chepil, 1950, Chepil and Woodruff, 1954). Spatial mapping of wind erosion susceptibility and upscaling the measured EF values to large scales is challenging, as there are several different contributing factors including soil, topography, meteorology factors.

DL is a promising technique for mapping different hazards at different scales (Shao et al., 2019). DL techniques has been successfully used in different studies for the spatial mapping of piping (Chen et al., 2021a), head-cut gully erosion (Band et al., 2020; Chen et al., 2021b; Saha et al., 2021), soil salinity (Mohammadifar et al., 2022), land subsidence (Li et al., 2021), and dust sources (Gholami et al., 2021a; Gholami et al., 2021b; Gholami and Mohammadifar, 2022). DL is a new method in aeolian studies, and to date there is no study on the use of DL for the estimation of soil susceptibility to wind erosion. Shallow ML models transform the inputs only one or two times, while DL models transform the inputs multiple times before delivering the outputs. As a

* Corresponding authors.
E-mail addresses: mahrooz.rezaei@wur.nl (M. Rezaei), hgholami@hormozgan.ac.ir (H. Gholami).

https://doi.org/10.1016/j.catena.2023.106953
Received 20 October 2022; Received in revised form 14 December 2022; Accepted 11 January 2023
Available online 23 January 2023

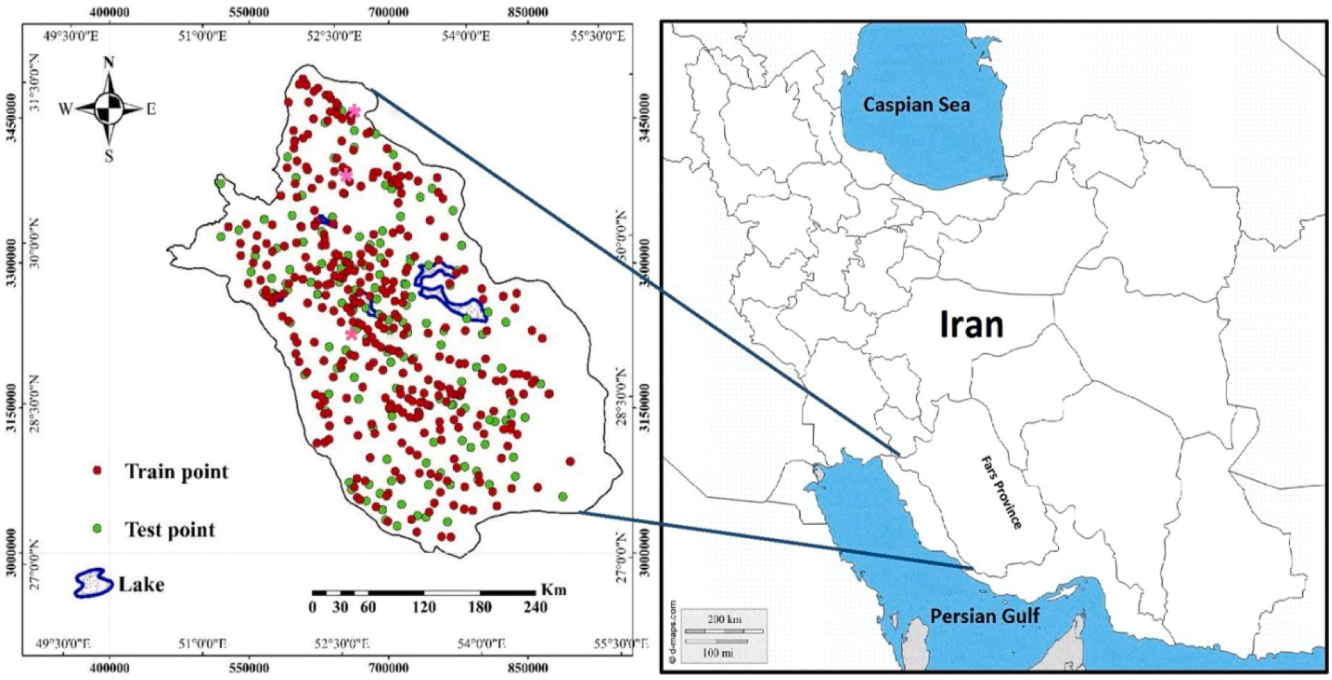

Fig. 1. The geographical location of Fars Province in Iran. Points are showing the locations of training samples, test samples and meteorological locations.

result, DL models can learn more complicated patterns, allowing end-to-end learning without manual feature engineering. In comparison with other techniques for studying wind erosion (e.g., erosion pins, field-based techniques), machine learning models are inexpensive and provide a basis for mapping provenance over large spatial scales.

Interpretability is one of the aspects one should consider when using DL models. Game theory is a method to interpret the predictive model output (including data mining (DM), ML and DL models) through two measures consisting of Shapley additive explanations (SHAP) and the Permutation Feature Importance Measure (PFIM) (Mohammadifar et al., 2021). Recently, the uncertainties involved with the DL and traditional machine learning models have been gaining increased attention (Hubschneider et al., 2019). The uncertainty of the predictions by DL models originates from different sources such as input data, model structure, etc. Therefore, quantifying the uncertainty of the DL models is a key step for successful modelling in different fields.

Iran is constantly exposed to dust storm events. The growing area susceptible to wind erosion and dust emission in Iran calls for immediate action. However, the picture of occurrence and scope of wind erosion in Iran is still unclear. Spatial maps of areas susceptible to wind erosion is missing, while this information is essential to better quantify wind erosion and apply the most practical mitigation measures. The first step in wind erosion mitigation is identifying the areas susceptible to wind erosion hazard. This is especially important for developing countries like Iran where limited soil conservation budgets are available and incorrect decision making by policy makers in prioritizing areas for the application of wind erosion mitigation measures may introduce irreparable costs. Therefore, this study aimed to better assess the areas that are susceptible to wind erosion using an easily measurable soil property (EF) based on extensive field work data and deep learning models. Such practical methodology is essential for mapping wind erosion on large scale. The main aims of our study are 1) determining the important and non-important variables controlling EF by the Repeated Elastic Net Technique (RENT) method; 2) predicting EF calculated by Chepil equation using the bidirectional gated recurrent unit (BiGRU) and bidirectional recurrent neural networks (BiRNN); 3) assessing the interpretability of prediction models with the help of game theory; and 4) quantifying the uncertainty of the predicted EF by DL model using deep quantile regression (DQR).

2. Material and methods

2.1. Study area

The study area was Fars province, southern Iran (27°2′ to 31°42′ latitude and 50°42′ to 55°36′ longitude). The area of Fars province is 133,299 km^2 with arid and semi-arid climate (Rezaei et al., 2022). The 3 meteorological stations of the province including Abadeh, Eghlid, and Shiraz are shown in Fig. 1. Dust storm is a common aeolian process in this province with the most intense ones recorded on 13 May 2018, 28 August 2013, 28 February 2009, 24 April 2008, 13 August 2001, and 17 July 1988 (Abbasi et al., 2021).

2.2. Field work and soil analysis

For this study, 508 soil samples were collected in different geographical locations of the Fars province. Soil sampling was done in the summer of 2019 and samples were collected from the surface soil (0–3 cm) which is prone to wind erosion. After sieving and air drying, the aggregate mean weight (MWD), organic matter and calcium carbonate equivalent (CCE) were measured by dry sieving method (Kemper and Rosenau, 1986), LOI method (Hoogsteen et al., 2015), and back titration method (Nelson, 1983), respectively. Besides, Bulk Density (BD) data was downloaded from the global database (soilgrids.org) and was mapped as a mosaic in GIS with a resolution of 50 * 50 m.

In addition to soil sampling, some soil properties were measured in the field including the resistance to penetration (PR) and the soil surface roughness (SR) using the pocket penetrometer (ELE model) (Bradford, 1986) and the chain method (Saleh, 1993), respectively. Five replicate experiments were considered for these measurements. SR was calculated by the following equation:

$$R = (1 - \frac{L2}{L1}) * 100 \quad (1)$$

where L1 is the chain length and L2 is the horizontal distance.

IDW (Inverse distance weighting) interpolation was used in ArcGIS for integrating the variation in different soil properties affecting the EF. The output maps are presented in Fig. 2. Identifying and mapping factors

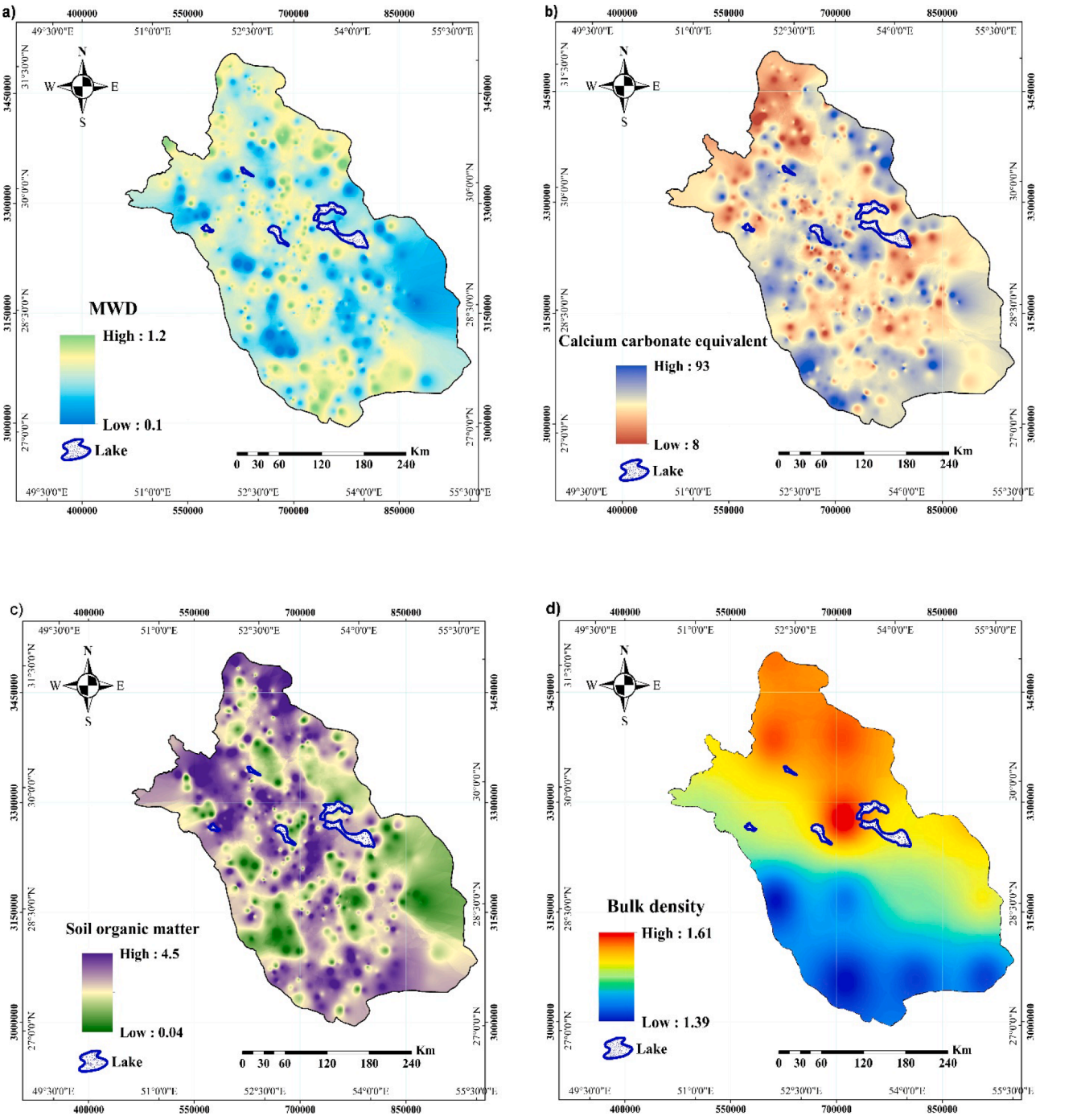

Fig. 2. Maps of soil factors influencing EF: a) Mean weight diameter (MWD), b) CCE, c) OM, d) Bulk density (BD), e) PR, and f) SR.

controlling EF as input data for the modelling process has the potential to yield accurate predictive maps for large scales. The main strength of the current study was therefore the use of high-resolution input data for mapping EF generated based on fieldworks.

2.3. EF inventory map

For assessing the relationship between EF and its controlling factors, 508 soil samples were collected and EF was calculated by using the Chepil method (Chepil, 1950) and the following equation:

$$EF = \frac{W_{<0.84}}{W_{total}} \times 100 \quad (2)$$

where EF is the wind erodible fraction of soil (%), $W_{<0.84}$ is the mass of aggregates smaller than 0.84 mm (g), and W_{total} is the total mass of soil sample (g). Fig. 2 presents the spatial maps of all measured soil properties. For constructing predictive models of EF, 356 samples (70 %) and 152 samples (30 %) were randomly selected as train and test datasets, respectively.

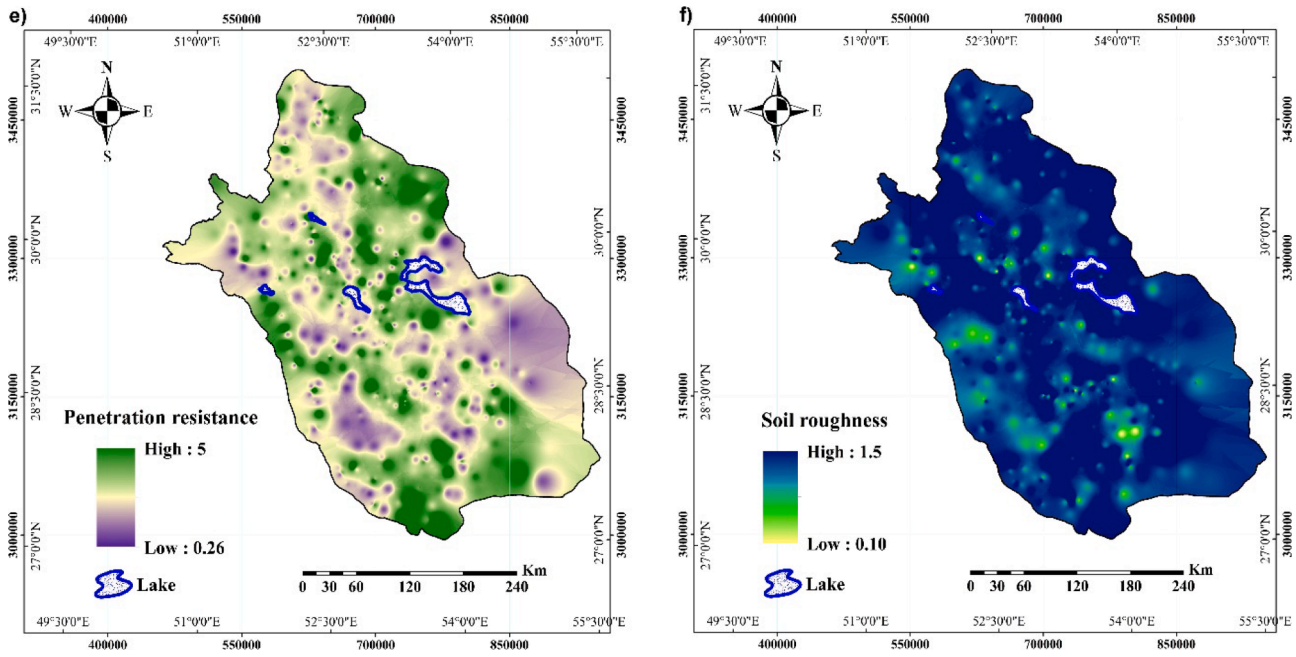

Fig. 2. (*continued*).

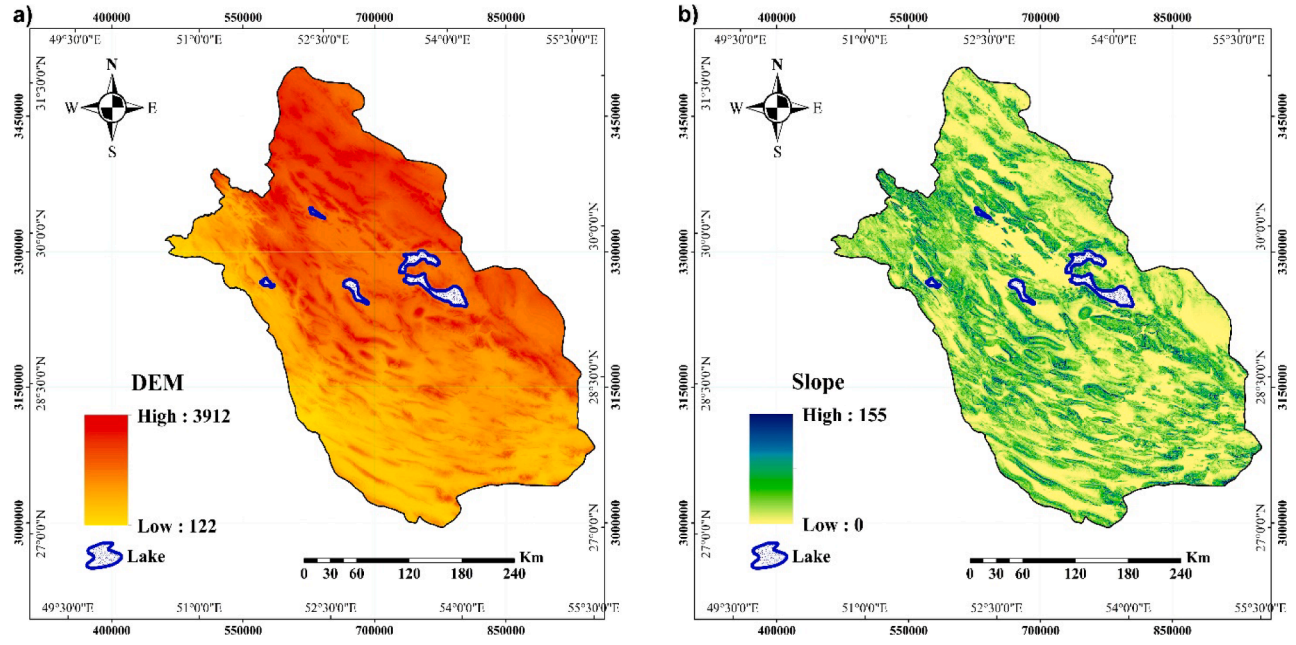

Fig. 3. Maps of topographic and meteorological factors influencing the EF: a) DEM, b) Slope, c) Wind speed (m/s), d) Precipitation (mm), and e) Evaporation (mm).

2.4. Mapping non-soil factors controlling EF

2.4.1. Topographic factors

The digital elevation model (DEM) was extracted from the website of USGS (earthexplorer.usgs.gov) with a 30 m × 30 m spatial resolution. Slope map was prepared from DEM using ArcGIS with the same spatial resolution.

2.4.2. Meteorological factors

The meteorological variables of wind velocity, precipitation, and evaporation for the period of 2010–2020 were mapped using the data of meteorological stations located in the study area and the Kriging method.

2.4.3. Other factors

Normalized difference vegetation index (NDVI) was produced from the Moderate Resolution Imaging Spectroradiometer (MODIS) satellite (MOD13Q1). NDVI has a spatial and temporal resolutions of 250 m and 16-day, respectively. Maps of land use (2019), soil order, and lithology were produced based on the maps taken form the Forest, Rangeland and Watershed Management Organization of Iran (IFRWMO), the Geological Survey and Mineral Exploration of Iran (GSMEI). Land was classified

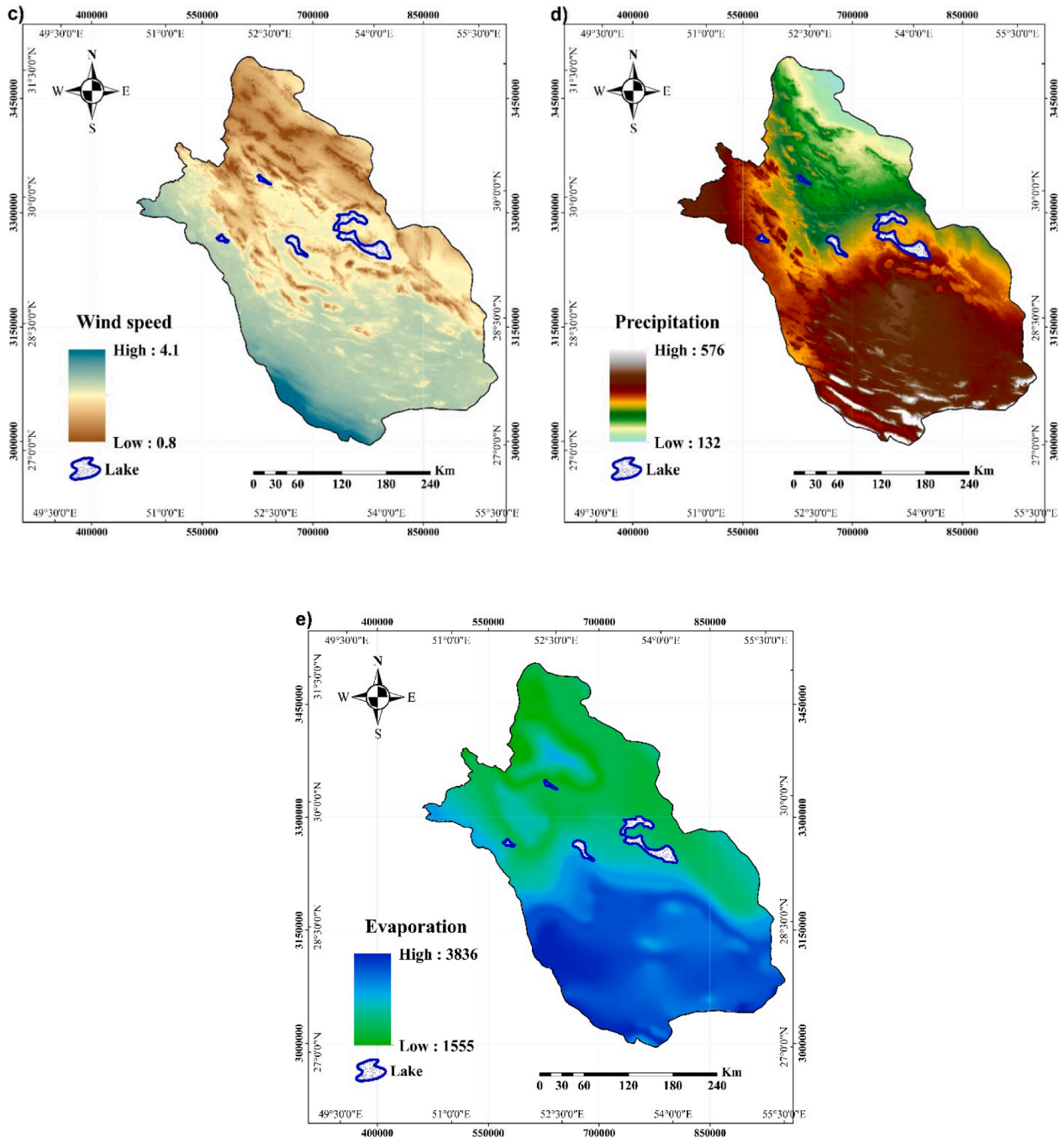

Fig. 3. (*continued*).

into no rocky outcrops and vegetation cover, agricultural lands, lakes, salt lands, forests, wetlands, water bodies, wood lands, and residential regions. For increasing the accuracy of the land use maps, Google Earth images and the ArcBruTile plugin were used.

All the input layers of EF in this study were transformed to a similar spatial resolution (50 × 50 m). The maps of all effective factors for EF are presented in Figs. 3 and 4.

2.5. Selecting important controlling variables

In this study, we first used a Kalman filter and then applied the Repeated Elastic Net Technique (RENT) for discriminating the important and non-important variables controlling EF. Detailed description of RENT is provided in Jenul et al. (2021). RENT uses an ensemble of generalized linear models with elastic net regularization, each trained on distinct subsets of the training data. Furthermore, unlike established feature selectors, RENT provides valuable information for model interpretation concerning the identification of objects in the data that are difficult to predict during training.

2.6. Mapping of EF by BiGRU and BiRNN models

For constructing predictive models of EF, 356 samples (70 %) and 152 samples (30 %) were randomly selected as train and test datasets, respectively. The EF maps was then produced using the selected controlling variables and overlapped using the BiGUR and BiRNN models. The Gated Recurrent Unit (GRU) – an updated version of RNN (Cho et al., 2014) - introduces a “gate mechanism” to update information on

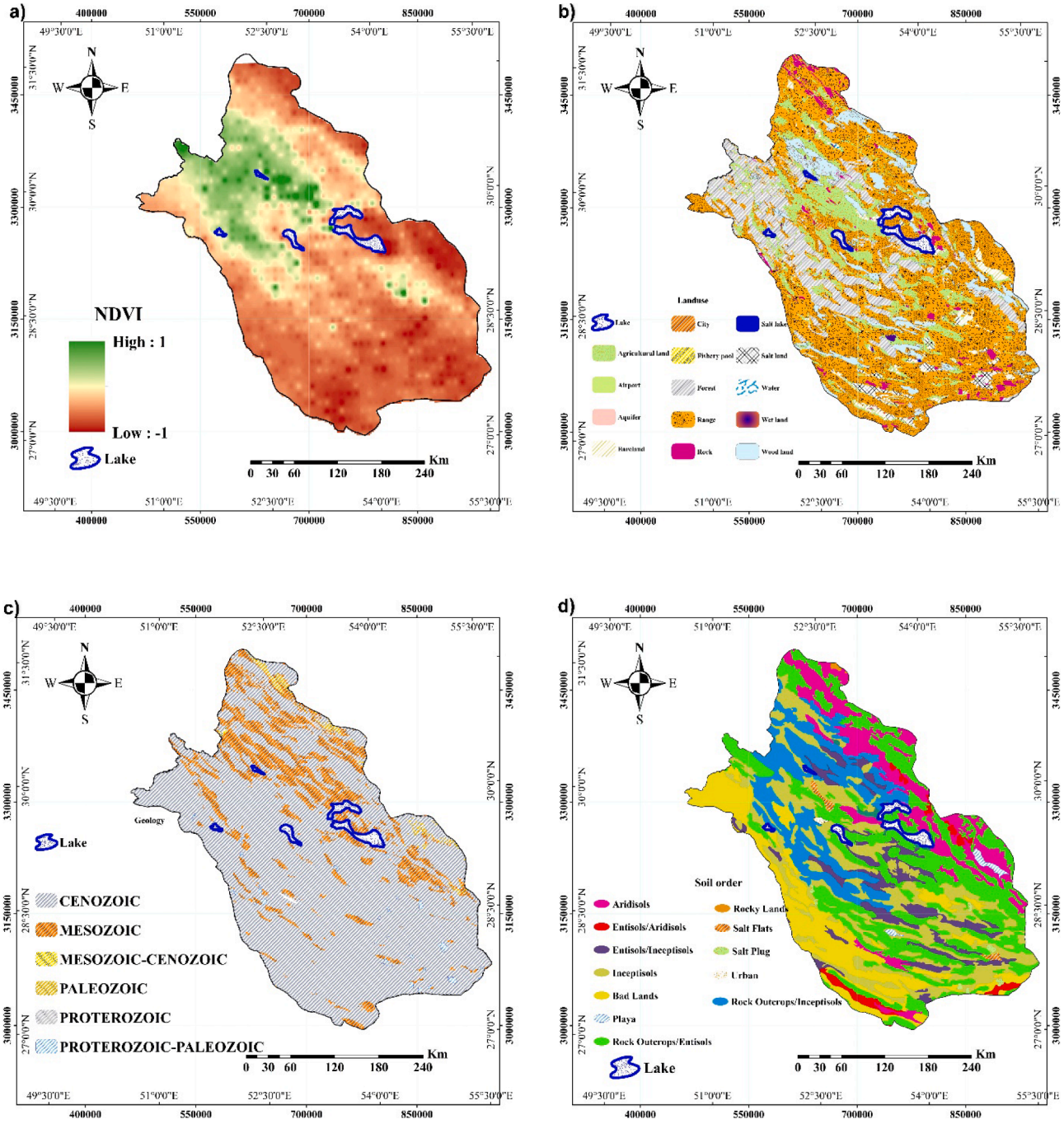

Fig. 4. Maps of other factors influencing the EF: a) NDVI, b) land use, c) geology, and d) soil order.

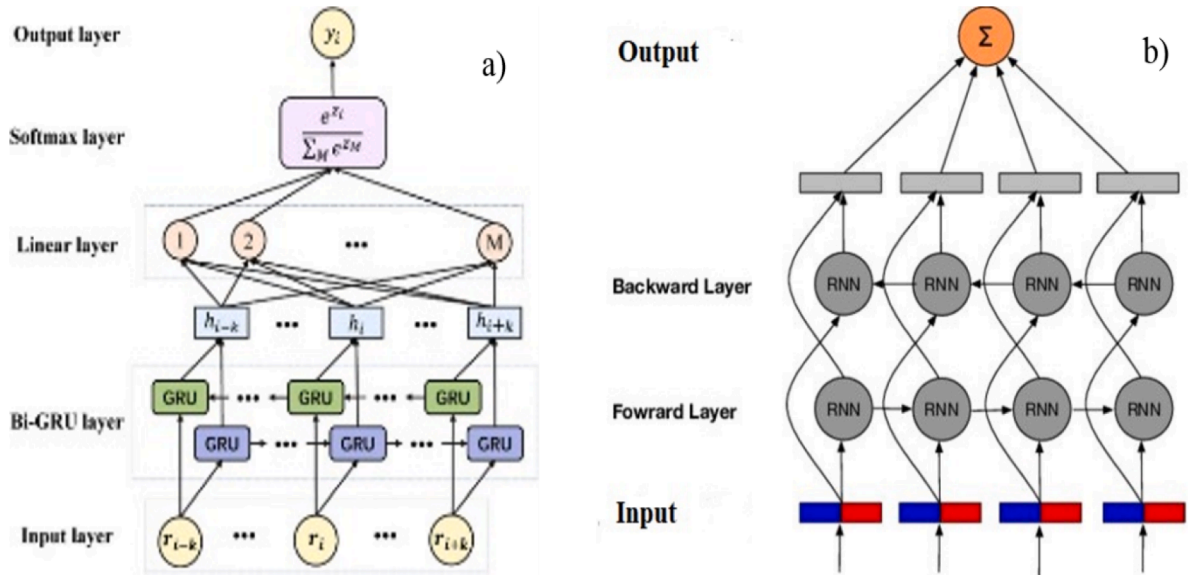

Fig. 5. The network structures for (a) BiGRU, and (b) BiRNN.

the basis of the RNN. The GRU consists the reset (rt) and update (zt) gates (Pan et al., 2020). We can express these gates, new memories (hti) and hidden state (ht) as follows (Mohammadifar et al., 2021):

$$rt = \sigma\ (W(r)\ xt + U(r)\ ht\text{-}1) \quad (3)$$

$$zt = \sigma\ (W(z)\ xt + U(z)\ ht\text{-}1) \quad (4)$$

$$hti = tanh\ (rt\ o\ Uht\text{-}1 + Wxt) \quad (5)$$

$$ht = (1 - zt)\ o\ hti + zt\ o\ ht\text{-}1 \quad (6)$$

where σ(.) is a sigmoid function, and W(r) and W(z) indicate weight matrices. Here, we used the bidirectional GRU (BiGRU) and bidirectional RNN (BiRNN) for predicting EF in the Fars province. The fundamental architecture of BiGRU networks consists of just putting together two separate GRUs (Abdelgwad et al., 2021). The network structure for the two models used to map EF is presented in Fig. 5.

2.7. Model evaluation

The Taylor diagram consisting of the correlation coefficient (r), the standard deviation (SD) and the root mean square error (RMSE), was used for assessing model performances (Taylor, 2001).

2.8. Assessment of the interpretability and uncertainty of DL models

The relative contribution of effective variables in EF prediction was determined by two measures of game theory including PFIM (Breiman, 2001) and SHAP (Lundberg and Lee (2017). Features were classified as "important" or "unimportant", by permutating the values and controlling whether model error was increased or had no change, respectively (Mohammadifar et al., 2021). SHAP values show the feature contribution in the final model predictions. For uncertainty analysis, quantile regression (QR) (Koenker and Bassett, 1978) was used, which is a least-square method in linear regression. Here, DeepQuantreg was applied to quantify uncertainty of the DL predictive model of EF.

All the steps for EF prediction using the combined modelling approach are presented in Fig. 6.

3. Results and discussion

3.1. Statistical parameters of soil properties

The statistical summary of the EF and some soil physicochemical properties are presented in Table 1. The bulk density of the studied soils was between 1.41 and 1.58 g cm^{-3} with an average of 1.51 g cm^{-3}, which indicates soils with different textures, confirming different wind erosion potential (Mina et al., 2022) across the study area. The soils were rich in CCE (mean = 53.58 %), which was related to the calcareous parent materials of southern Iran. The amount of organic matter in the study area was low; between 0.79 and 2.90 %, with an average of 2.02 %. Organic matter deficiency can reduce soil aggregation and increase soil erodibility. The EF had the highest coefficient of variation (CV = 22.47 %), showing different wind erosion potential in the study area.

3.2. Determining the important variables controlling EF

Based on the Kalman smoother filter and RENT method, seven variables including MWD, PR, precipitation, wind speed, land use, slope and OCC were the most important factors for controlling EF among the 15 factors examined. Factors of Bulk Density, CEC, Roughness, Evaporation, DEM, Lithology, NDVI and soil order were considered as unimportant parameters for EF prediction. The number of parameters selected by RENT for the studied dataset is low (less than half of the total parameters) which is indeed the strength of RENT method in terms of the interpretability of results. To have deeper insight into the properties of the dataset, the frequency of each variable is presented in the frequency plot (Fig. 7a). Based on the frequency plot, the order of the importance of variables were as follow: MWD > penetration resistance > precipitation > wind speed > land use > slope > organic carbon. Considering the correlation loadings plot (Fig. 7b), the importance of a variable in the explained variance is higher the further it is located from the center (Valbuena et al., 2013). The inner circle represents 50 % and the outer circle represents the 100 % of explained variances. In this plot, each point is one parameter in the plane spanned by component 1 and component 2. In fact, the loadings of correlation indicate the contribution of the selected parameters to the variance explained by components 1 and 2. 60.6 % of the total variance is explained by the first two principal components. Results were roughly consistent with the frequency plot except for organic matter which showed a higher priority here. The similarity between groups is also visible here (Fig. 7b) showing the classified soil, topographic and meteorological variables. In other words, it is evident that classified parameters are highly correlated as they are located so close to each other. From these results, it becomes clear that wind erosion is not only dependent on soil properties but also other factors including meteorology and topography play important roles.

MWD, penetration resistance and organic carbon are among the soil

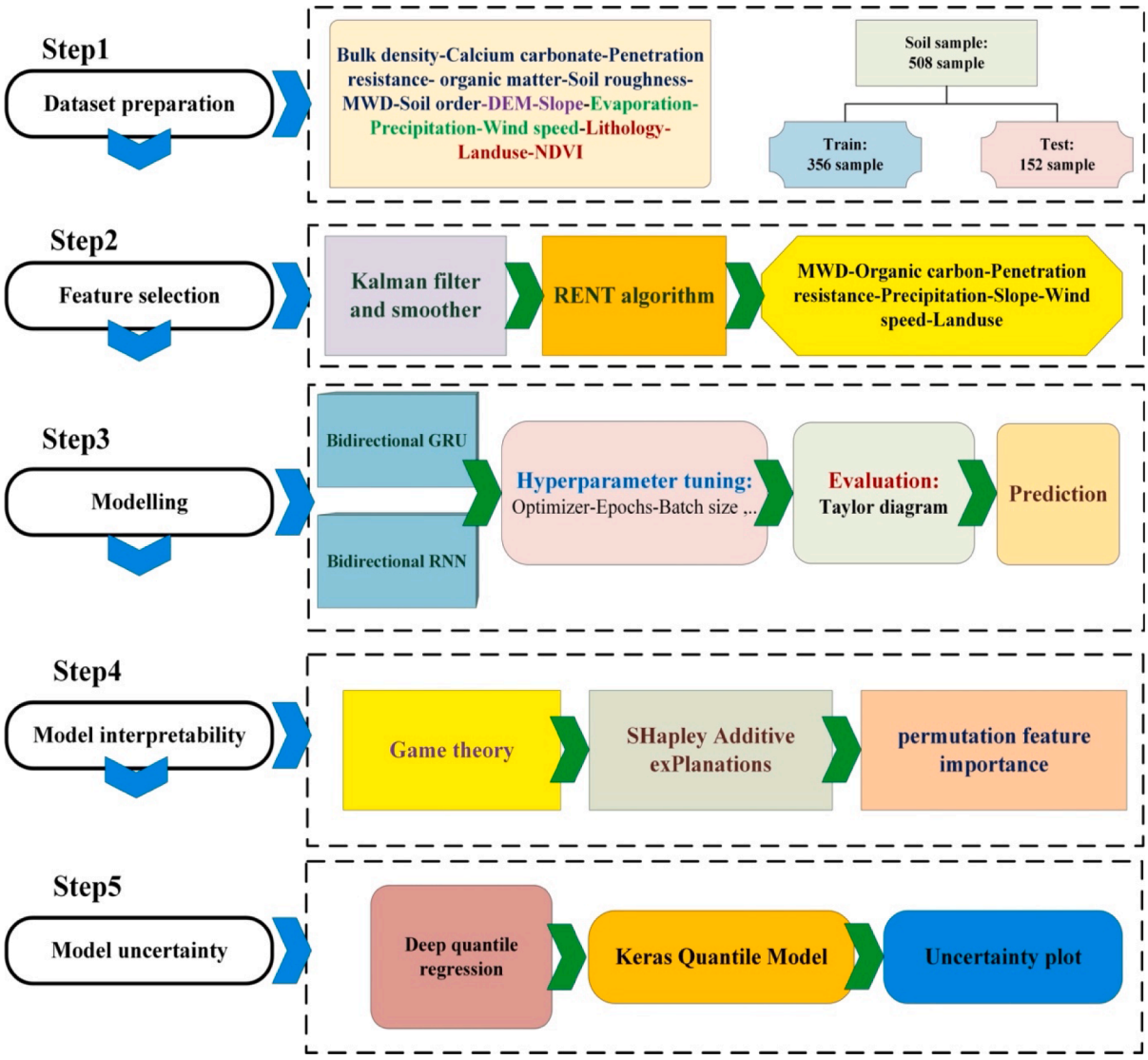

Fig. 6. Flowchart of the different stages in the spatial modeling of EF using DL. MWD – mean weight diameter; DEM; NDVI; RENT – repeated elastic net technique; GRU – gated recurrent units; RNN –recurrent neural networks.

Table 1
Statistical analysis of the soil properties and EF.

Soil property	Unit	Min.	Max.	Mean	STD	CV (%)
Target (EF)	%	17.63	100	66.87	15.02	22.47
Bulk density	gr cm^{-3}	1.41	1.58	1.51	0.05	3.36
Calcium carbonate	%	39.36	70	53.58	5.22	9.74
MWD	mm	0.45	0.94	0.73	0.08	11.46
Organic carbon	%	0.79	2.90	2.02	0.41	20.23
Penetration	Kg cm^{-2}	0.94	3.02	1.98	0.39	19.82
Roughness	cm	0.39	0.73	0.54	0.06	11.14

properties affecting soil erodibility by wind erosion. The positive effect of MWD on soil erosion reduction has been reported in many studies (Rezaei et al., 2022, Ciric et al., 2012). The more organic matter present in the soil, the higher the MWD which result in binding soil particles and decreasing soil erodible fraction (Villasica et al., 2018; Négyesi et al., 2016; Liu et al., 2007). Soil moisture is another preliminary factor for decreasing soil wind erosion and dust emission (Gholami et al., 2021a; Parajuli et al., 2019) as it can increase the adhesion between particles, which is reflected in the precipitation parameter.

Land use has also a significant effect on wind erosion and EF (Rezaei et al., 2016). Mozaffari et al. (2021) reported quantitatively how different land uses such as cultivated field, fallow field, rangeland, and orchard fields could change EF which is in line with our findings. Land use has also an indirect role as it has an impact on OM and soil biological activities altogether, they have an impact on the aggregate stability. Among the meteorological parameters, wind speed showed the highest correlation as expected and this was consistent with the study by Behrooz et al. (2017), who reported the strong influence of wind velocity on aeolian transport and dust emission in southeast of Iran. Slope was also selected as the main topographic parameter.

3.3. EF map generated by BiGRU and BiRNN models

The EF maps produced by BiGUR and BiRNN models are presented in Fig. 8ab. Both models were consistent in spatial distribution of the EF over the Fars province. Areas with yellowish colors show higher EF (>50 %) and thus are more sucecptible to wind eroison. A large part of the province in the south east shows high erodibility, which was also evident during field study as there were scarce vegetations (see Fig. 4a) and soils were very loose. One aspect that attracts attention is the low occurence of bluish colors (<40 % of EF) which indicates that most of the Fars province has moderate to high erodibility and thus our

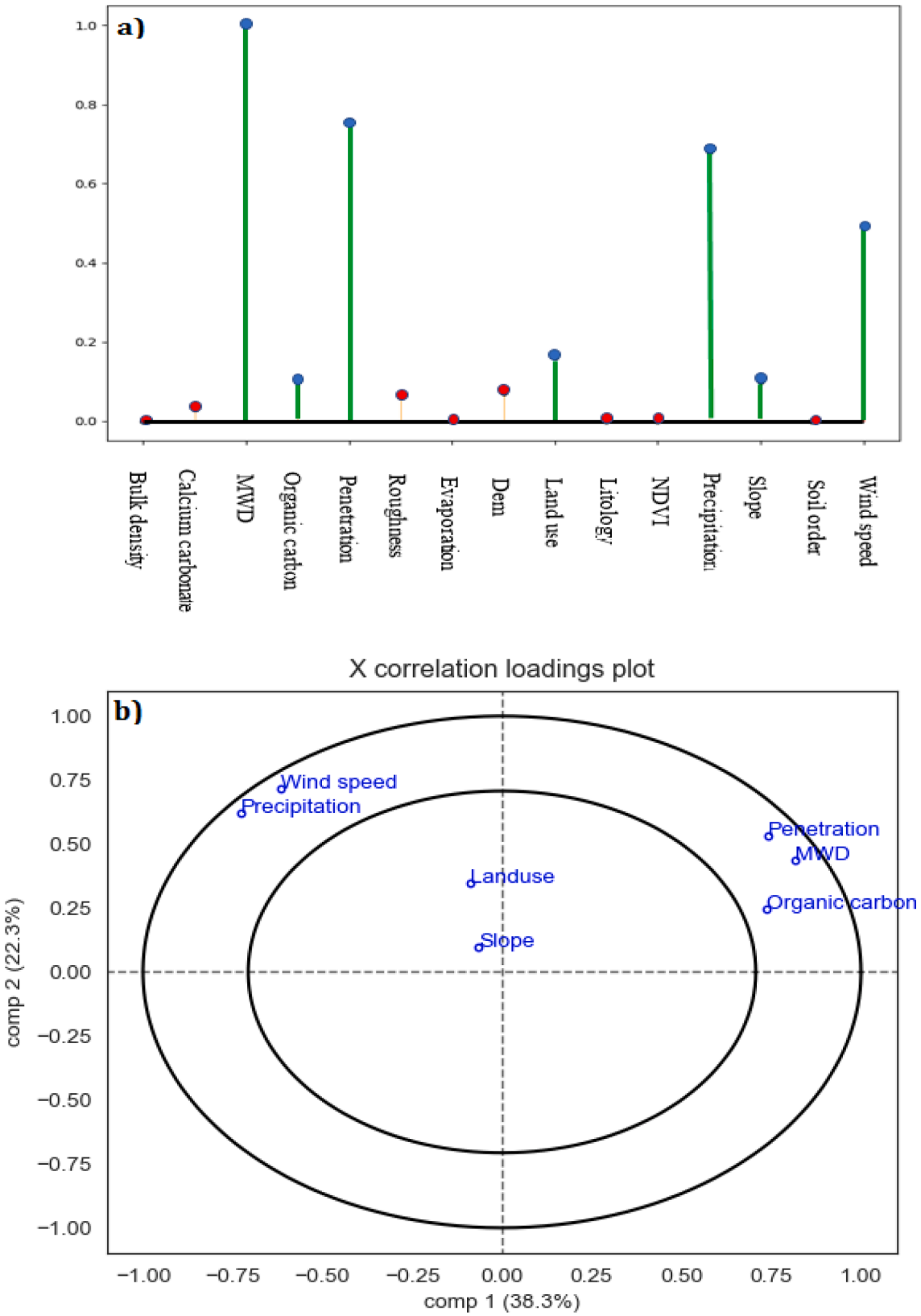

Fig. 7. Feature selection based on a) frequency plot and b) correlation loading plot for EF prediction.

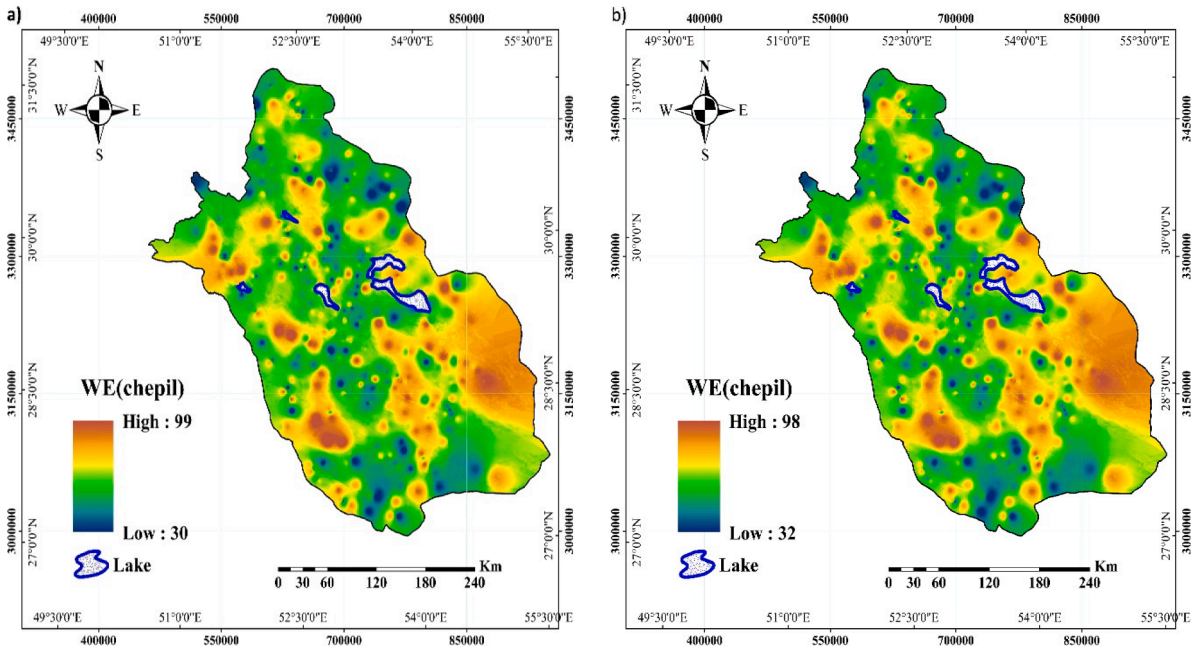

Fig. 8. Final EF maps generated by a) BiGRU and b) BiRNN models.

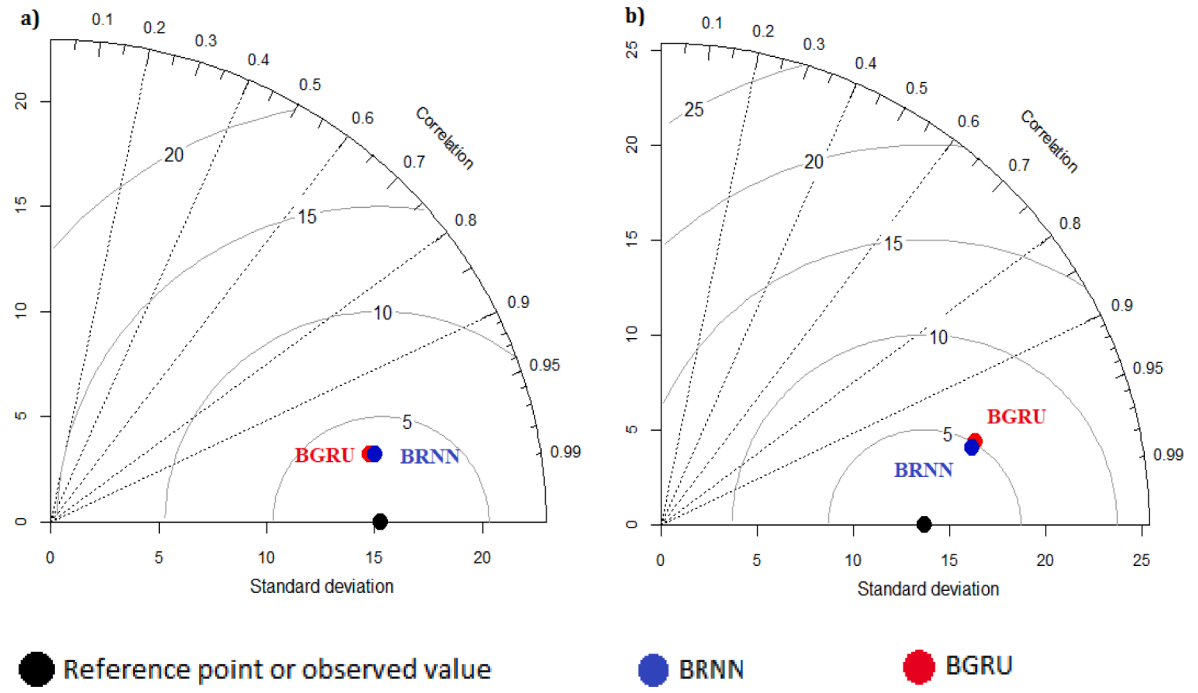

Fig. 9. Taylor diagram for assessing the performance of the models. a) training-dataset, b) test-dataset. BiGRU, BiRNN, and RMSE indicate the bidirectional Gated Recurrent Units, Bidirectional Recurrent Neural Network, and Root Mean Squared Error, respectively.

Table 2
Statistics of measured versus predicted EF using BiGRU, and BiRNN models.

Model	R^2		RMSE (%)	
	Train	Test	Train	Test
BiGRU	0.92	0.93	4.40	6.55
BiRNN	0.92	0.94	4.47	5.96

hypothesis about the critical situation of Fars province in terms of wind eroison is unfortunately accepted.

3.4. Assessment of model performance for predicting EF

Results for EF prediction using BiRNN and BiGRU models are summarized in Fig. 9, and Table 2. Based on the Taylor diagram (Fig. 9), the RMSE and the correlation coefficient (r) for both models and for both training and test datasets exceeded 0.9 and were<5 %, respectively. As presented in Table 2, the prediction accuracy of the two predictive models of BiRNN and BiGRU in the training dataset was very similar to

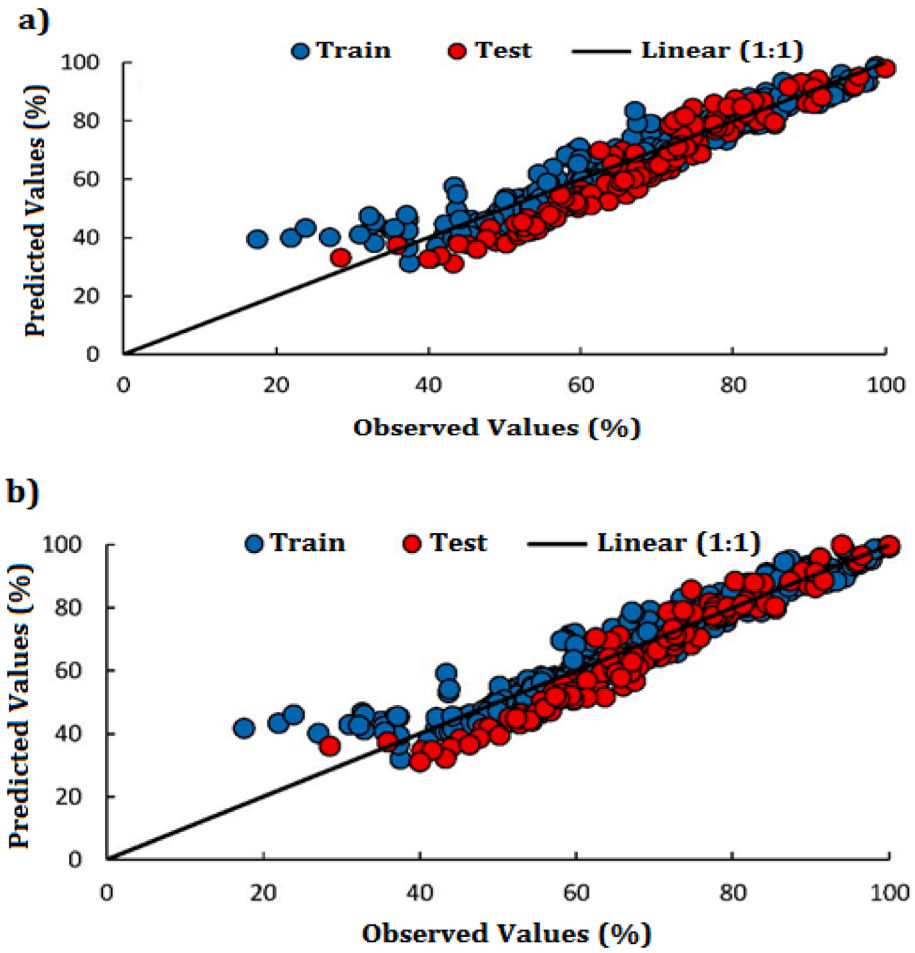

Fig. 10. Scatter plots of predicted values of measured EF by "Train" (N = 356) and "Test" dataset (N = 152) using a) BiGRU (bidirectional gated recurrent units), b) BiRNN (bidirectional recurrent neural network) models.

the observed value and only differed slightly in the amount of RMSE. In general, BiRNN showed slightly higher performance (R^2 = 0.94, RMSE = 5.96 %) than BiGRU (R^2 = 0.93, RMSE = 6.55 %) in the test dataset. The results of this study proved that DL models can predict EF accurately. Considering the high speed of computing of DL models, the problem of encountering large areas prone to wind erosion and dealing with big datasets are overcome.

Successful application of machine learning algorithms especially shallow learning models (e.g., support vector machine, frequency ratio, random forest, adaptive neuro-fuzzy inference system, cubist) in the field of wind erosion has been reported since 2020 (Gholami et al., 2020; Rahmati et al., 2020; Boroughani et al., 2020, Kouchami-Sardoo et al., 2020b). More recently, application of deep learning models has been introduced remarkably. The results of Gholami and Mohammadifar (2022) for classifying dust sources in the Middle East using two hybrid DL models (CNN-GRU and DLDL-RF) was consistent with our study.

Observed and predicted values of EF values using different models in both training and test sets are shown in Fig. 10. Training and test sets are well located around the 1:1 line which indicate the accountability of the estimate, since the measured and predicted values are largely consistent.

3.5. Interpretability of EF predictive models

The importance of controlling factors of EF and their contribution in the predictive model output were calculated using PFIM and SHAP, respectively (Fig. 11). The results of PFIM suggested the following decreasing order of importance: MWD > penetration > organic carbon > precipitation > wind speed > land use > slope. SHAP (Fig. 11b) combines factor importance with factor effects. The color represents the factor from low to high. Overlapping points are projected in the y-axis direction in order to find the distribution of the SHAP values per factor. The factors are ordered according to their importance. The contribution of each factor estimated using SHAP was: MWD > penetration > precipitation > wind speed > land use > slope > organic carbon. Overall, soil parameters especially MWD were selected as the most controlling parameter which was consistent with the results of PFIM.

Previous studies in the arid regions of Iran and worldwide (Mina et al., 2021; Kouchami-Sardoo et al., 2020a; Sirjani et al., 2019; Saadoud et al., 2018; Blanco-Canqui et al., 2009) reported that MWD, penetration, organic carbon, precipitation, and wind speed are among the major factors affecting soil wind erosion. Our results showed that game theory is a helpful technique for testing the interpretability of wind erosion models. Using SHAP and PFIM we could highlight the critical control factors for soil wind erosion and improve the interpretability of DM models.

3.6. Uncertainty associated with EF values predicted by BiRNN model

Fig. 12 shows the results of DQR including the upper band and lower bands of predicted EF versus observed EF. According to Fig. 12, the points of all models do follow a particular pattern and are randomly scattered around the horizontal axis, which indicates the suitability of the developed models for predicting the EF. Overall, the observed values fell within predictions provided by model indicating the high accuracy of the predictive model.

The uncertainty associated with EF prediction can originate from

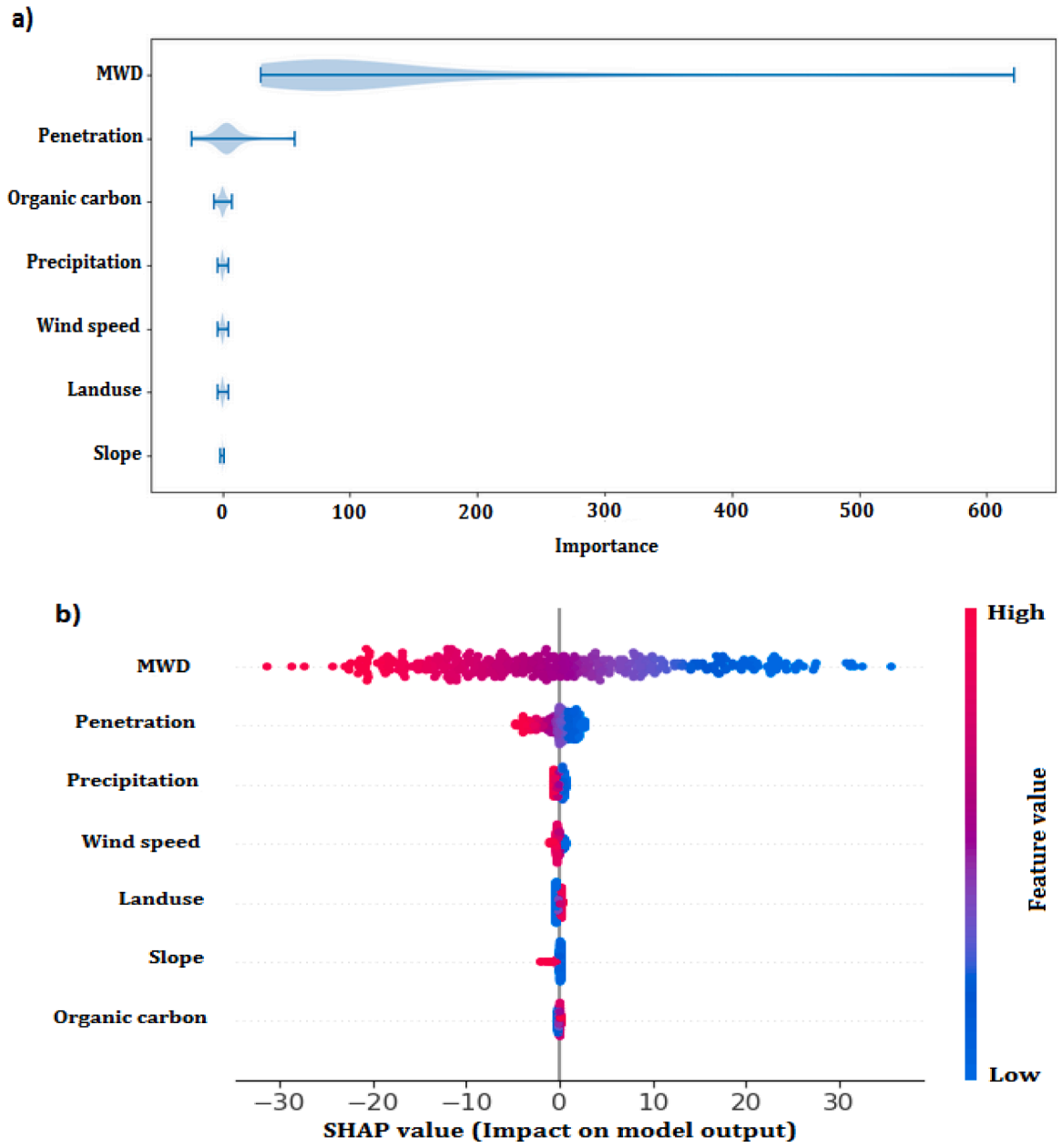

Fig. 11. A) the importance of the factors affecting the soilerodible fraction (EF) using the permutation feature importance measure (PFIM) and b) The contribution of factors to the predictive model output based on the Shapley additive explanations (SHAP) value.

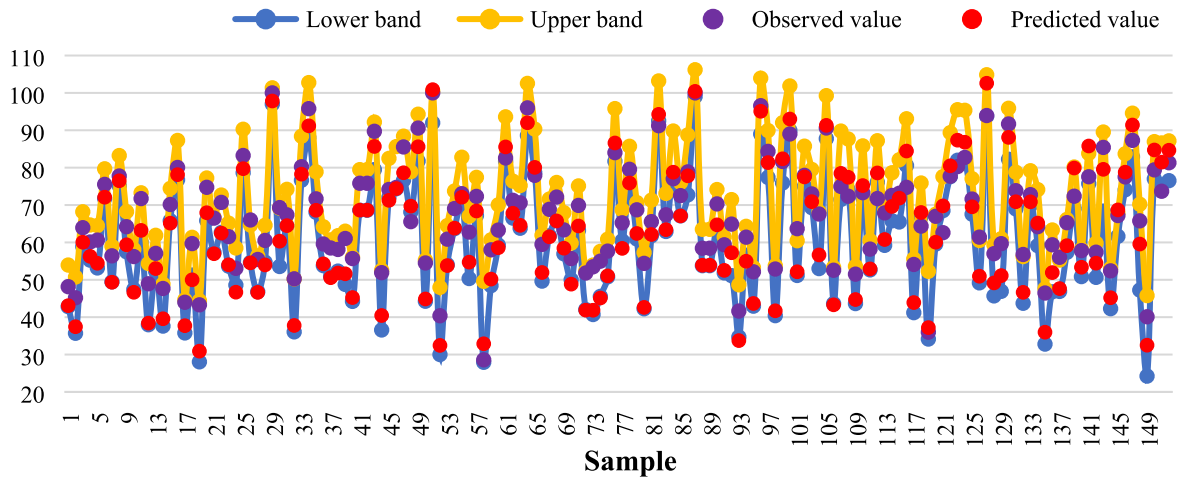

Fig. 12. Uncertainty associated with EF values predicted by the BiRNN model.

several sources. A principal limitation for EF estimation on large scale is the uncertainty associated with limited number of soil samples. In this study we provided enough data as input for prediction models (508 soil samples). Therefore, a high-density sampling with a suitable distribution is recommended. Higher accuracy of DL model might be achieved with higher spatial resolution of the imagery, as it can significantly improve some factors such as NDVI and DEM. Wind velocity and precipitation are also sensitive to the length of data records.

4. Conclusion

Accurate wind erosion assessment for large scales is still a challenge in dry and semi-arid environments especially for developing countries like Iran. There is lack of harmonized methodology for targeting areas susceptible to wind erosion effectively. The novelty of this work was the first-time use of deep learning algorithms for the spatial mapping of erodible fraction of soil, namely EF, which is an easily measurable soil property and a good index of soil susceptibility to wind erosion. The accuracy assessment confirmed good performance of DL models for spatial mapping of EF. The spatial distribution of soil susceptibility to wind erosion using EF index is produced, which can be used as a base for further integrated modelling of wind erosion. These maps provide insights for identifying areas at risk of wind erosion and can help policy-makers when considering soil conservation measures. We strongly propose to produce such a map for the whole country of Iran as wind erosion and dust emission is getting widespread and quick actions are urgent.

Declaration of Competing Interest

The authors declare that they have no known competing financial interests or personal relationships that could have appeared to influence the work reported in this paper.

Data availability

Data will be made available on request.

References

Abbasi, S., Rezaei, M., Keshavarzi, B., Mina, M., Ritsema, C., Geissen, V., 2021. Investigation of the 2018 Shiraz dust event: Potential sources of metals, rare earth elements, and radionuclides; health assessment. Chemosphere 279, 130533.

Abdelgwad, M.M., Soliman, T.H.A., Taloba, A.I., Farghaly, M.F., 2021. Arabic aspect based sentiment analysis using bidirectional GRU based models. J. King Saud Univ.-Comput. Inform. Sci.

Band, S.S., Janizadeh, S., Chandra Pal, S., Saha, A., Chakrabortty, R., Shokri, M., Mosavi, A., 2020. Novel ensemble approach of deep learning neural network (DLNN) model and particle swarm optimization (PSO) algorithm for prediction of gully erosion susceptibility. Sensors 20 (19), 5609.

Behrooz, R.D., Esmaili-Sari, A., Bahramifar, N., Kaskaoutis, D.G., Saeb, K., Rajaei, F., 2017. Trace-element concentrations and water-soluble ions in size-segregated dust-borne and soil samples in Sistan, southeast Iran. Aeolian Res. 25, 87–105.

Blanco-Canqui, H., Mikha, M.M., Benjamin, J.G., Stone, L.R., Schlegel, A.J., Lyon, D.J., Stahlman, P.W., 2009. Regional study of no-till impacts on near-surface aggregate properties that influence soil erodibility. Soil Sci. Soc. Am. J. 73 (4), 1361–1368.

Boroughani, M., Pourhashemi, S., Hashemi, H., Salehi, M., Amirahmadi, A., Asadi, M.A. Z., Berndtsson, R., 2020. Application of remote sensing techniques and machine learning algorithms in dust source detection and dust source susceptibility mapping. Eco. Inform. 56, 101059.

Borrelli, P., Ballabio, C., Panagos, P., Montanarella, L., 2014. Wind erosion susceptibility of European soils. Geoderma 232, 471–478.

Bradford, J.M., 1986. Penetrability. Methods Soil Anal.: Part 1 Phys. Mineral. Methods 5, 463–478.

Breiman, L., 2001. Random forests. Mach. Learn. 45 (1), 5–32.

Chen, Y., Chen, W., Janizadeh, S., Bhunia, G.S., Bera, A., Pham, Q.B., Wang, X., 2021b. Deep learning and boosting framework for piping erosion susceptibility modeling: spatial evaluation of agricultural areas in the semi-arid region. Geocarto Int. 1–27.

Chen, W., Lei, X., Chakrabortty, R., Pal, S.C., Sahana, M., Janizadeh, S., 2021a. Evaluation of different boosting ensemble machine learning models and novel deep learning and boosting framework for head-cut gully erosion susceptibility. J. Environ. Manage. 284, 112015.

Chepil, W.S., 1950. Properties of soil which influence wind erosion: 11. Dry aggregate structure as an index of erodibility. Soil Sci 69, 403–414.

Chepil, W.S., 1962. A compact rotary sieve and the importance of dry sieving in physical soil analysis. Soil Sci. Soc. Am. J. 26 (1), 4–6.

Chepil, W.S., Woodruff, N.P., 1954. Estimations of wind erodibility of field surfaces. J. Soil Water Conserv 9 (257–265), 285.

Cho, K., Van Merriënboer, B., Gulcehre, C., Bahdanau, D., Bougares, F., Schwenk, H., & Bengio, Y. (2014). Learning phrase representations using RNN encoder-decoder for statistical machine translation. *arXiv preprint arXiv:1406.1078*.

Ciric, V., Manojlovic, M., Nesic, L., Belic, M., 2012. Soil dry aggregate size distribution: effects of soil type and land use. J. Soil Sci. Plant Nutr. 12 (4), 689–703.

Gholami, H., Mohamadifar, A., Collins, A.L., 2020. Spatial mapping of the provenance of storm dust: Application of data mining and ensemble modelling. Atmos. Res. 233, 104716.

Gholami, H., Mohammadifar, A., Golzari, S., Kaskaoutis, D.G., Collins, A.L., 2021a. Using the Boruta algorithm and deep learning models for mapping land susceptibility to atmospheric dust emissions in Iran. Aeolian Res. 50, 100682.

Gholami, H., Mohammadifar, A., Malakooti, H., Esmaeilpour, Y., Golzari, S., Mohammadi, F., Collins, A.L., 2021b. Integrated modelling for mapping spatial sources of dust in central Asia-An important dust source in the global atmospheric system. Atmos. Pollut. Res. 12 (9), 101173.

Gholami, H., Mohammadifar, A., 2022. Novel deep learning hybrid models (CNN-GRU and DLDL-RF) for the susceptibility classification of dust sources in the Middle East: a global source. Sci. Rep. 12 (1), 1–12.

Hoogsteen, M.J., Lantinga, E.A., Bakker, E.J., Groot, J.C., Tittonell, P.A., 2015. Estimating soil organic carbon through loss on ignition: effects of ignition conditions and structural water loss. Eur. J. Soil Sci. 66 (2), 320–328.

Hubschneider, C., Hutmacher, R., Zöllner, J.M., 2019. Calibrating uncertainty models for steering angle estimation. In: 2019 IEEE intelligent transportation systems conference (ITSC). IEEE, pp. 1511-1518.

Jenul, A., Schrunner, S., Huynh, B.N., Tomic, O., 2021. RENT: A Python package for repeated elastic net feature selection. J. Open Source Software 6 (63), 3323.

Kemper, W.D., Rosenau, R.C., 1986. Aggregate stability and size distribution. In: Klute, A. Ed., Methods of soil analysis. Part 1. Agronomy Monograph 9. 2nd ed., Madison, Wisconsin, 425-442.

Koenker, R., Bassett Jr, G., 1978. Regression quantiles. Econometrica 33–50.

Kouchami-Sardoo, I., Shirani, H., Besalatpour, A.A., 2020a. Determining the Features Influencing the Structural Stability of Soils of Arid Regions Using a Hybrid GA-ANN Algorithm. Appl. Soil Res. 8 (3), 129–143.
Kouchami-Sardoo, I., Shirani, H., Esfandiarpour-Boroujeni, I., Besalatpour, A.A., Hajabbasi, M.A., 2020b. Prediction of soil wind erodibility using a hybrid Genetic algorithm–Artificial neural network method. Catena 187, 104315.
Li, H., Zhu, L., Dai, Z., Gong, H., Guo, T., Guo, G., Wang, J., Teatini, P., 2021. Spatiotemporal modeling of land subsidence using a geographically weighted deep learning method based on PS-InSAR. Sci. Total Environ. 799, 149244.
Liu, L.Y., Li, X.Y., Shi, P.J., Gao, S.Y., Wang, J.H., Ta, W.Q., Xiao, B.L., 2007. Wind erodibility of major soils in the farming-pastoral ecotone of China. J. Arid Environ. 68 (4), 611–623.
Lundberg, S.M., Lee, S.I., 2017. A unified approach to interpreting model predictions. Adv. Neural Inf. Proces. Syst. 30.
Mina, M., Rezaei, M., Sameni, A., Moosavi, A.A., Ritsema, C., 2021. Vis-NIR spectroscopy predicts threshold velocity of wind erosion in calcareous soils. Geoderma 401, 115163.
Mina, M., Rezaei, M., Sameni, A., Ostovari, Y., Ritsema, C., 2022. Predicting wind erosion rate using portable wind tunnel combined with machine learning algorithms in calcareous soils, southern Iran. J. Environ. Manage. 304, 114171.
Mohammadifar, A., Gholami, H., Comino, J.R., Collins, A.L., 2021. Assessment of the interpretability of data mining for the spatial modelling of water erosion using game theory. Catena 200, 105178.
Mohammadifar, A., Gholami, H., Golzari, S., 2022. Assessment of the uncertainty and interpretability of deep learning models for mapping soil salinity using DeepQuantreg and game theory. Sci. Rep. 12 (1), 1–12.
Mozaffari, H., Rezaei, M., Ostovari, Y., 2021. Soil sensitivity to wind and water erosion as affected by land use in southern Iran. Earth 2 (2), 287–302.
Négyesi, G., Lóki, J., Buró, B., Szabó, S., 2016. Effect of soil parameters on the threshold wind velocity and maximum eroded mass in a dry environment. Arab. J. Geosci. 9 (11), 1–10.
Nelson, R.E., 1983. Carbonate and gypsum. Methods Soil Anal.: Part 2 Chem. Microbiol. Properties 9, 181-197.
Pan, E., Mei, X., Wang, Q., Ma, Y., Ma, J., 2020. Spectral-spatial classification for hyperspectral image based on a single GRU. Neurocomputing 387, 150–160.
Parajuli, S.P., Stenchikov, G.L., Ukhov, A., Kim, H., 2019. Dust emission modeling using a new high-resolution dust source function in WRF-Chem with implications for air quality. J. Geophys. Res. Atmos. 124 (17–18), 10109–10133.
Rahmati, O., Panahi, M., Ghiasi, S.S., Deo, R.C., Tiefenbacher, J.P., Pradhan, B., Bui, D. T., 2020. Hybridized neural fuzzy ensembles for dust source modeling and prediction. Atmos. Environ. 224, 117320.
Rezaei, M., Mina, M., Ostovari, Y., Riksen, M.J., 2022. Determination of the threshold velocity of soil wind erosion using a wind tunnel and its prediction in calcareous soils of Iran. Land Degradation Develop.
Rezaei, M., Sameni, A., Shamsi, S.R.F., Bartholomeus, H., 2016. Remote sensing of land use/cover changes and its effect on wind erosion potential in southern Iran. PeerJ 4, e1948.
Rezaei, M., Riksen, M.J., Sirjani, E., Sameni, A., Geissen, V., 2019. Wind erosion as a driver for transport of light density microplastics. Sci. Total Environ. 669, 273–281.
Saadoud, D., Hassani, M., Peinado, F.J.M., Guettouche, M.S., 2018. Application of fuzzy logic approach for wind erosion hazard mapping in Laghouat region (Algeria) using remote sensing and GIS. Aeolian Res. 32, 24–34.
Saha, A., Pal, S.C., Arabameri, A., Chowdhuri, I., Rezaie, F., Chakrabortty, R., Roy, P., Shit, M., 2021. Optimization modelling to establish false measures implemented with ex-situ plant species to control gully erosion in a monsoon-dominated region with novel in-situ measurements.“. J. Environ. Manage. 287, 112284.
Saleh, A., 1993. Soil roughness measurement: chain method. J. Soil Water Conserv. 48 (6), 527–529.
Shao, W., Ge, Z., Song, Z., Wang, K., 2019. Nonlinear industrial soft sensor development based on semi-supervised probabilistic mixture of extreme learning machines. Control Eng. Pract. 91, 104098.
Shao, Y., Klose, M., Wyrwoll, K.H., 2013. Recent global dust trend and connections to climate forcing. J. Geophys. Res. Atmos. 118 (19), 11–107.
Sirjani, E., Sameni, A., Moosavi, A.A., Mahmoodabadi, M., Laurent, B., 2019. Portable wind tunnel experiments to study soil erosion by wind and its link to soil properties in the Fars province, Iran. Geoderma 333, 69–80.
Středová, H., Podhrázská, J., Chuchma, F., Středa, T., Kučera, J., Fukalová, P., Blecha, M., 2021. The Road Map to Classify the Potential Risk of Wind Erosion. ISPRS Int. J. Geo Inf. 10 (4), 269.
Taylor, K.E., 2001. Summarizing multiple aspects of model performance in a single diagram. J. Geophys. Res. Atmos. 106 (D7), 7183–7192.
Valbuena, R., Packalen, P., Mehtätalo, L., García-Abril, A., Maltamo, M., 2013. Characterizing forest structural types and shelterwood dynamics from Lorenz-based indicators predicted by airborne laser scanning. Can. J. For. Res. 43 (11), 1063–1074.
Villasica, L.J., Lina, S., Asio, V., 2018. Aggregate stability affects carbon sequestration potential of different tropical soils. Ann. Trop. Res 40, 71–88.